

# Growth and band gap of strained $\langle 110 \rangle$ $\text{Si}_{1-x}\text{Ge}_x$ layers on silicon substrates by chemical vapor deposition

C. W. Liu and J. C. Sturm

*Department of Electrical Engineering, Princeton University, Princeton, New Jersey 08544*

Y. R. J. Lacroix and M. L. W. Thewalt

*Department of Physics, Simon Fraser University, Burnaby, British Columbia V5A 1S6, Canada*

D. D. Perovic

*Department of Metallurgy and Material Science, University of Toronto, Toronto, Ontario M5S 1A4, Canada*

(Received 17 January 1994; accepted for publication 2 May 1994)

We report chemical vapor deposition growth of strained  $\text{Si}_{1-x}\text{Ge}_x$  alloy layers on  $\langle 110 \rangle$  Si substrates. Compared to the same growth conditions on  $\langle 100 \rangle$  substrates, a slightly lower Ge composition and a much lower growth rate was observed. From photoluminescence measurements, the band gap of these films for  $0.16 \leq x \leq 0.43$  is evaluated and compared to theory. Finally, a surprisingly large “no-phonon” replica line strength ratio was observed as compared with that observed in  $\langle 100 \rangle$  layers.

Strained  $\text{Si}_{1-x}\text{Ge}_x/\text{Si}$  heterojunctions grown commensurately on  $\text{Si}\langle 100 \rangle$  substrates have been widely investigated, but very little work has been done on this material system for other substrate orientations. Because of the different effects of strain on the conduction-band minima in  $\text{Si}_{1-x}\text{Ge}_x$  (which do not lie at the  $\Gamma$  point), changing the direction of strain can have dramatic effects on the electronic properties on the resulting films. For example, in strained  $\text{Si}_{1-x}\text{Ge}_x$  films on  $\langle 100 \rangle$  Si substrates, four conduction-band minima move down in energy and two move up, on  $\langle 110 \rangle$  substrates the opposite is predicted, and on  $\langle 111 \rangle$  substrates all six are predicted to remain degenerate.<sup>1</sup> Furthermore, the maximum conduction-band offset (for type I alignment) between strained  $\text{Si}_{1-x}\text{Ge}_x$  and Si on  $\langle 110 \rangle$  substrates is predicted to be substantially larger than that on  $\langle 100 \rangle$  substrates. We therefore have investigated the growth of these films on  $\langle 110 \rangle$  substrates. We report the growth of such  $\langle 110 \rangle$   $\text{Si}_{1-x}\text{Ge}_x$  films by chemical vapor deposition (CVD), and the thorough measurement of their band gaps.

Previous work in  $\langle 110 \rangle$   $\text{Si}_{1-x}\text{Ge}_x$  includes a structural study of samples grown by molecular beam epitaxy (MBE),<sup>2</sup> electron intersubband transition on relaxed SiGe buffers by MBE,<sup>3</sup> and one photoluminescence report of a single sample also grown by MBE.<sup>4</sup> All the  $\langle 110 \rangle$  samples reported in this letter were grown on 100-mm wafers (except sample 1361 which was grown on a 75-mm wafer) by rapid thermal chemical vapor deposition (RTCVD). The Si layers were grown at a nominal temperature of 700 °C from dichlorosilane, and the  $\text{Si}_{1-x}\text{Ge}_x$  layers were grown at a nominal temperature of 625 °C from germane and dichlorosilane. The growth temperature was accurately measured on all samples by infrared transmission with an estimated error of  $\pm 5$  °C,<sup>5</sup> except on sample 1361. An anomalously low growth temperature on sample 1361 may explain the unexpectedly large Ge fraction on that sample. The growth pressure was 6 Torr, the gas flows were 3 standard liters per minute (slpm) for a hydrogen carrier and 26 sccm for dichlorosilane, and the germane mixture flow (0.8% in hydrogen) varied from 100 to 450 sccm. The details of the RTCVD reactor can be found

in Ref. 5. For samples characterized by photoluminescence, the  $\text{Si}_{1-x}\text{Ge}_x$  layers were capped with  $\sim 100$  Å of silicon. Previous experiments on  $\langle 100 \rangle$  samples in our lab have shown that a Si cap increases the photoluminescence intensity by over an order of magnitude, presumably due to a decrease in surface recombination.<sup>6</sup>

The thickness of  $\text{Si}_{1-x}\text{Ge}_x$  quantum wells in the photoluminescence sample were measured by cross-sectional transmission electron microscopy (XTEM). Using this thickness, and the integrated atomic areal density of Ge from Rutherford backscattering spectroscopy (RBS), assuming that atomic density of  $\text{Si}_{1-x}\text{Ge}_x$  is a linear function of Ge content, and assuming abrupt interfaces, we obtained the Ge content in the quantum wells. The measured Ge content and quantum well thickness of each sample is summarized in Table I. Both the Ge content and the growth rate increase as germane flow increases (Fig. 1). Compared to  $\langle 100 \rangle$  Si substrates, the same growth conditions yielded  $\text{Si}_{1-x}\text{Ge}_x$  layers with a slightly lower Ge content, but much lower growth rates (a factor of 2–3 lower). The Ge content was also determined from x-ray diffraction, using (440) peaks on thick  $\text{Si}_{1-x}\text{Ge}_x$  layers ( $>0.5$   $\mu\text{m}$ ), which were grown under the same conditions and annealed at 900 °C for more than 3 h to promote relaxation. Assuming complete relaxation, this method yielded Ge fractions 10% to 20% relatively higher than that obtained from RBS and XTEM. The inconsistency may be due to a much lower dislocation density along  $[\bar{1}\bar{1}0]$  direction on (110) substrates,<sup>2</sup> which could cause insufficient relaxation on the thick samples. The strained  $\text{Si}_{1-x}\text{Ge}_x$  layers were observed by XTEM to be abrupt within 0.3–0.4 nm, similar to  $\langle 100 \rangle$  layers of similar thickness grown either by CVD or MBE techniques.<sup>7</sup> Moreover, all of the quantum wells were defect-free on the scale of XTEM.

The 4- and 77-K photoluminescence (PL) were taken with samples immersed in liquid helium and liquid nitrogen, respectively. The excitation source was an  $\text{Ar}^+$  ion laser. At 4 K, the PL spectrum of a 23-Å strained  $\langle 110 \rangle$   $\text{Si}/\text{Si}_{0.57}\text{Ge}_{0.43}/\text{Si}$  quantum well [Fig. 2(a)] is qualitatively similar to what has been reported in  $\langle 100 \rangle$  substrates,<sup>8,9</sup> and presumably due to

TABLE I. Summary of the quantum well samples used in the study. The thickness is measured from cross-sectional TEM. The Ge composition ( $x$ ) is determined by the combination of cross-sectional TEM and RBS.  $E_{g,PL}$  and  $r_{np}$  are obtained from photoluminescence. The quantum confinement energy ( $\Delta E_{conf}$ ) is calculated from the conditions of a square potential profile, a theoretical valence band discontinuity  $\Delta E_v = 0.71x$  (see Ref. 1), the measured quantum well thickness, the hole effective mass of  $0.28 m_0$  (see Ref. 12), and the electron effective mass of  $0.19 m_0$ . The  $E_g$  is the band gap after quantum confinement corrections. The uncertainty in  $E_{g,PL}$  is from fitting the PL spectra, and the uncertainty in  $\Delta E_{conf}$  is from the uncertainty in the quantum well thickness.

Sample No.	Thickness ( $\text{\AA}$ )	$x$	$E_{g,PL}$ (eV)	$r_{np}$	$\Delta E_{conf}$ (eV)	$E_g$ (eV)
1361	$23 \pm 3$	$0.43 \pm 0.08$	$0.947 \pm 0.005$	2.66	$0.110 \pm 0.029$	$0.837 \pm 0.029$
1463	$51 \pm 3$	$0.29 \pm 0.02$	$0.916 \pm 0.005$	3.15	$0.059 \pm 0.007$	$0.857 \pm 0.009$
1464	$62 \pm 4$	$0.26 \pm 0.02$	$0.957 \pm 0.005$	2.06	$0.041 \pm 0.005$	$0.916 \pm 0.007$
1465	$127 \pm 4$	$0.21 \pm 0.01$	$0.973 \pm 0.005$	1.51	$0.013 \pm 0.001$	$0.96 \pm 0.005$
1466	$106 \pm 4$	$0.16 \pm 0.01$	$1.017 \pm 0.005$	1.0	$0.016 \pm 0.002$	$1.001 \pm 0.005$

shallow bound exciton recombination. The strongest peak in the spectrum is the no-phonon (NP) transition due to the lattice disorder (alloy fluctuations, interface roughness, and impurities) which relaxes the momentum conservation requirement. Similar to that observed in  $\langle 100 \rangle$  wells,<sup>8</sup> there are four phonon-assisted replicas at the lower energy side of the NP line, which are attributed to the transverse acoustical (TA) phonon and the three transverse optical (TO) phonon replicas related to Si-Si, Si-Ge, and Ge-Ge vibrations. Only a few of the quantum wells exhibited such strong well-resolved band-edge luminescence at 4 K, while all of them exhibited band-edge luminescence at 77 K. The reason for this effect is not clear, but may be related to nonradiative traps due to an intermittent vacuum integrity or gas purity problem in the CVD reactor. In any case, this effect was also observed in samples grown on  $\langle 100 \rangle$  substrates at the same time frame as these samples, so it is not unique to the  $\langle 110 \rangle$  orientation. As a result, the band gaps were extracted from the 77-K PL spectra. The 77-K PL spectrum (pump-power density  $\sim 20 \text{ W/cm}^2$ ) for the same sample of Fig. 2(a) is shown in Fig. 2(b). At 77 K, thermal broadening and a band-filling effect due to the pump-power lead to broad overlapping peaks [Figs. 2(b)–2(e)]. To extract a band gap, the 77-K PL spectra were fitted using an electron-hole plasma model (EHP).<sup>10</sup> The model convolves the ideal line shape for a single electron-hole transition over all the occupied electron

and hole states. Assuming constant matrix elements for both NP lines and phonon replicas for all possible transitions, all transitions in the EHP were accounted for by the following integral:

$$I(h\nu) = I_0 \int_0^{h\nu - E_{g,PL}} dE D_e(E) D_h(h\nu - E_{g,PL} - E) \times f(E, F_e, T) f(h\nu - E_{g,PL} - E, F_h, T), \quad (1)$$

where  $D_e$  and  $D_h$  are the densities of states of electrons and holes, respectively,  $h\nu$  is the photon energy,  $E_{g,PL}$  is the PL band gap, and  $f$  is the Fermi function for electrons and holes. The electron Fermi energy  $F_e$  and hole Fermi energy  $F_h$  are determined by carrier densities and linked through charge neutrality. To model the shape from each possible electron-hole transition, the relative ratios of the different TO transitions (Si-Si, Si-Ge, Ge-Ge) were taken from the statistical bond counting model of Weber and Alonso,<sup>11</sup> and the phonon energies of Ref. 11 were used. The line shape due to each possible electron-hole transition was then convolved with Eq. (1), which represents all possible electron-hole transitions. The three adjustable parameters in fitting the line shape

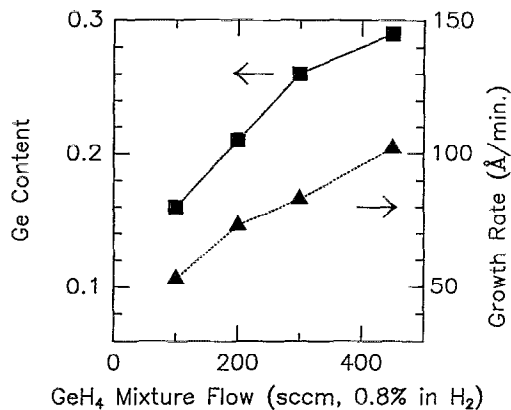


FIG. 1. Growth rate and Ge composition for strained  $\text{Si}_{1-x}\text{Ge}_x$  growth on  $\langle 110 \rangle$  Si substrates vs germane mixture flow (0.8% in hydrogen) (sample 1463–1466). The growth temperature was  $625^\circ\text{C}$  and the pressure is 6 Torr with 26 sccm dichlorosilane and 3 slpm hydrogen flows.

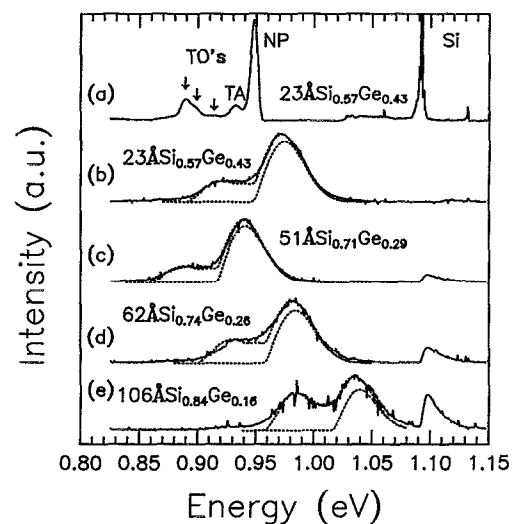


FIG. 2. PL spectra of strained  $\langle 110 \rangle$   $\text{Si}/\text{Si}_{1-x}\text{Ge}_x/\text{Si}$  quantum wells measured at (a) 4 K and (b)–(e) 77 K. The dotted lines in (b)–(e) are the theoretical fitting of electron-hole plasma model and the no-phonon component of the model. The onsets of the no-phonon lines at the low-energy side are the band gaps of the quantum wells,  $E_{g,PL}$ .

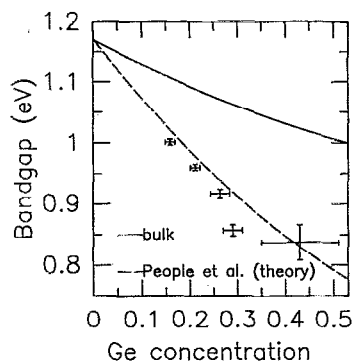


FIG. 3. The plot of band gap ( $E_g$  in Table I) vs Ge content for  $\text{Si}_{1-x}\text{Ge}_x$  strained on  $\langle 110 \rangle$  Si substrates. The dotted line is the theoretical prediction of People *et al.* for  $\langle 110 \rangle$  Si substrates (Ref. 13). The solid line is the relaxed band gap from Ref. 11 with the addition of 15 meV for exciton binding energy.

were the band gap ( $E_{g,PL}$ ), the ratio of the NP line strength to the total strength of TO lines ( $r_{np}$ ), and the sum of  $F_e + F_h$  (which affects the linewidth). The fitted spectra are shown in Fig. 2. Also shown in Fig. 2 are the contributions from the NP lines only. The band gap,  $E_{g,PL}$ , is the lower edge of this component, and was found to be fairly insensitive to all of the other fitting parameters, and also insensitive to variations in the assumed relative strengths of the various TO transitions. A summary of the fitting results for different samples is shown in Table I. Note that the band-gap value obtained from 77-K PL of Fig. 2(b) is very close to the energy position of NP line (excitonic band gap) in 4-K PL [Fig. 2(a)] of the same sample. To determine the “true band gap” of strained  $\langle 110 \rangle$   $\text{Si}_{1-x}\text{Ge}_x$ , we have to calculate the quantum confinement energies of both holes and electrons. We assumed a square potential profile, a theoretical valence band discontinuity  $\Delta E_v = 0.71x$ ,<sup>1</sup> the measured quantum well thickness, the hole effective mass of  $0.28 m_0$ ,<sup>12</sup> and the electron effective mass of  $0.19 m_0$ . Figure 3 displays a plot of the band gap of strained  $\langle 110 \rangle$   $\text{Si}_{1-x}\text{Ge}_x$  versus Ge content after corrections for quantum confinement. The data are very close to the theoretical curve of People *et al.*,<sup>13</sup> which is plotted in Fig. 3 for comparison along with the band gap of bulk  $\text{Si}_{1-x}\text{Ge}_x$ .<sup>11</sup> Although the band gap of strained  $\text{Si}_{1-x}\text{Ge}_x$  on  $\langle 110 \rangle$  substrates is predicted to be slightly lower than that on  $\langle 100 \rangle$  substrates [approximately 15 meV lower for  $x=0.4$  (Ref. 1)], within experimental resolution of  $E_g$  and  $x$ , we can not observe such a shift in a comparison of the 77-K PL of  $\langle 100 \rangle$  and  $\langle 110 \rangle$  samples grown in our lab.

Finally, it is interesting to note that in these  $\langle 110 \rangle$  strained layers, the integrated NP/TO ratio was substantially stronger than that observed in comparable  $\langle 100 \rangle$  structures.

For example, sample 1463 ( $x=0.29$ ) had a NP/TO ratio,  $r_{np}$ , of 3.2, extracted from the PL spectrum at 77 K. For a sample of similar composition on  $\langle 100 \rangle$  substrates, we typically observed  $r_{np} \sim 1.6$ . In the 4-K spectra [Fig. 2(a)], the relative height of the NP line was also about twice that in similar  $\langle 100 \rangle$  samples. The no-phonon photoluminescence transition in indirect band-gap semiconductors can be attributed to alloy scattering, interface roughness scattering, or localization of excitons by impurities (although the latter should not be significant at 77 K when excitons are not bound at impurities). Whether the alloy scattering is affected by the different strain in  $\langle 100 \rangle$  versus  $\langle 110 \rangle$  samples, or whether the interface roughness is substantially different is not known. Further investigation of this effect, which may lead to enhanced no-phonon transition rates for optical devices, is in progress.

In summary, we have reported the growth of strained  $\langle 110 \rangle$   $\text{Si}_{1-x}\text{Ge}_x$  by CVD, and used the photoluminescence spectroscopy to measure the band gap of strained  $\langle 110 \rangle$   $\text{Si}_{1-x}\text{Ge}_x$  on Si. Our results are in good agreement with the prediction of People *et al.*,<sup>13</sup> but the small predicted difference between the band gap of films strained on  $\langle 110 \rangle$  versus  $\langle 100 \rangle$  substrates has not been resolved within experimental error. Finally, the no-phonon luminescence of the  $\langle 110 \rangle$  films is relatively stronger than that on  $\langle 100 \rangle$  substrates, but the physical origin of this effect is not understood.

The RBS assistance of H. Gossmann (AT&T Bell Labs) and A. St Amour (Princeton University), and the support of ONR (N00014-90-J-1316) and NSF are gratefully appreciated. The work of Simon Fraser University was supported by the National Science and Engineering Research Council of Canada.

- <sup>1</sup>C. G. Van de Walle and R. M. Martin, Phys. Rev. B **34**, 5621 (1986).
- <sup>2</sup>R. Hull, J. C. Bean, L. Peticolas, and D. Bahnick, Appl. Phys. Lett. **59**, 964 (1991).
- <sup>3</sup>C. Lee and K. L. Wang, Appl. Phys. Lett. **60**, 2264 (1992).
- <sup>4</sup>S. Fukatsu, N. Usami, and Y. Shiraki, Jpn. J. Appl. Phys. **32**, 1502 (1993).
- <sup>5</sup>J. C. Sturm, P. V. Schwartz, E. J. Prinz, and H. Manoharan, J. Vac. Sci. Technol. B **9**, 2011 (1991).
- <sup>6</sup>J. C. Sturm, X. Xiao, P. V. Schwartz, and C. W. Liu, J. Vac. Sci. Technol. B **10**, 1998 (1992).
- <sup>7</sup>D. D. Perovic, G. C. Weatherly, and D. C. Houghton, Philos. Mag. **64**, 1 (1991).
- <sup>8</sup>J. C. Sturm, H. Manoharan, L. C. Lenchyshyn, M. L. W. Thewalt, N. L. Rowell, J.-P. Noël, and D. C. Houghton, Phys. Rev. Lett. **66**, 1362 (1991).
- <sup>9</sup>D. J. Robbins, L. T. Canhan, S. J. Barnett, A. D. Pitt, and P. Calcott, J. Appl. Phys. **71**, 1407 (1992).
- <sup>10</sup>X. Xiao, C. W. Liu, J. C. Sturm, L. C. Lenchyshyn, and M. L. W. Thewalt, Appl. Phys. Lett. **60**, 1720 (1992).
- <sup>11</sup>J. Weber and M. I. Alonso, Phys. Rev. B **40**, 5683 (1989).
- <sup>12</sup>X. Xiao, C. W. Liu, J. C. Sturm, L. C. Lenchyshyn, M. L. W. Thewalt, R. B. Gregory, and P. Fejes, Appl. Phys. Lett. **60**, 2135 (1992).
- <sup>13</sup>R. People, J. C. Bean, and D. V. Lang, in *Semiconductors and Semimetals*, Vol. 32, *Strained-Layer Superlattice: Physics*, edited by T. P. Pearsall (Academic, New York, 1990), p. 141.